ЕҢБЕК ҚЫЗЫЛ ТУ ОРДЕНДІ
«Ә. Б. БЕКТҰРОВ АТЫНДАҒЫ
ХИМИЯ ҒЫЛЫМДАРЫ ИНСТИТУТЫ»
АКЦИОНЕРЛІК ҚОҒАМЫ

ҚАЗАҚСТАННЫҢ ХИМИЯ ЖУРНАЛЫ

ХИМИЧЕСКИЙ ЖУРНАЛ КАЗАХСТАНА

CHEMICAL JOURNAL of KAZAKHSTAN

АКЦИОНЕРНОЕ ОБЩЕСТВО
ОРДЕНА ТРУДОВОГО КРАСНОГО ЗНАМЕНИ
«ИНСТИТУТ ХИМИЧЕСКИХ НАУК
им. А. Б. БЕКТУРОВА»

3 (67)

ИЮЛЬ – СЕНТЯБРЬ 2019 г.

ИЗДАЕТСЯ С ОКТЯБРЯ 2003 ГОДА

ВЫХОДИТ 4 РАЗА В ГОД

АЛМАТЫ
2019

UDC546.661

ZH. S. SHALABAYEV, A. K. OSKENBAY,
P. E. ORAZBAY, A. SH. DUISENKULOVA

Al-Farabi Kazakh national university, Almaty, Republic of Kazakhstan

SYNTHESIS OF CuS/S NANOCOMPOSITES BY HYDROTHERMAL WAY AND THEIR CHARACTERIZATION

Abstract. Copper sulfide/sulfur nanocomposites have been successfully synthesized by hydrothermal route reacting $Cu(CH_3COO)_2$, $CuCl_2$and $(NH_2)_2CS$ in aqua media at 80 °C. The synthesized sample was studied by X-ray diffraction (XRD), Raman spectroscopy, TG-DS, and scanning electron microscopy (SEM) analysis. According to the results of XRD analysis, the diffraction peaks of the CuS/S nanocomposites closely matched the standard copper sulfide and sulfur peaks. The average crystallite size of copper sulfide and sulfur particles was about 3.5 and 3.6 nm, respectively. Results of TG-DSC analysis showed that composite material contains about 16.16 % of sulfur and 12.29 % of copper sulfide (covellite). SEM images presented that composite material consists of two different microstructures: elongated needle-like and non-structured agglomerates.

Keywords: copper sulfide, sulfur, nanocomposite, hydrothermal route, shape control.

Introduction. In addition to the synthesis of semiconductor nanoparticles, which are used for various purposes(e.g. in solar cells, cathode material in lithium batteries, optical filters, or in photocatalysis) [1, 2], the synthesis of binary[3, 4], ternary [5] and quaternary nanocomposites[6-8] based on them is intensively studied. This is explained by the fact that nanocomposites, unlike nanoparticles, have a wider range of application fields and improved properties [5, 9-11].

Copper sulfide nanoparticles are promising materials for electrical and optical applications, as well as for biomedical ones [12-15]. In the work of Wang et al. [16] nanocomposites on the basis, copper sulfide nanoparticles were used for antibacterial application, and they could completely kill the *E. coli* cells through damaging the cell walls.

There are many preparation methods of copper sulfide nanoparticles such as sonochemical method [17], microwave irradiation method [18], molecular template method [19], polyol route [20], chemical vapour deposition [21], mechanochemical synthesis [22]and hydrothermal method [23, 24].

Sulfur nanoparticles are suitable for similar applications like copper sulfide nanoparticles, namely their use in lithium battery [25-27] and pharmaceutical technologies are of importance. This comes from its anti-cancer, antibacterial and antifungal activities [28-32]. Sulfur nanoparticles can be synthesized by the different preparation methods such as electrochemical method [33], microemulsion technique [34], aqueous surfactant solutions [35, 36], ultrasonic treatment of sulfur-cystine solution [37], oxidation H_2S gas using Fe-chelate [34],acid hydrolysis of sodium thiosulphate[38].

CuS/S nanocomposite might exhibit interesting properties utilizing the beneficial characteristics of the two components. This has been already demonstrated in [39, 40].

In this study, we have synthesized binary nanocomposites CuS/S via a hydrothermal route, which is simple and cost-efficient.

MATERIALS AND METHODS

Copper acetate monohydrate – $Cu(CH_3COO)_2 \times H_2O$, copper chloride – $CuCl_2 \times 2H_2O$ and thiourea – $(NH_2)_2CS$ were purchased from Laborpharma Co. Ltd. (Almaty, Kazakhstan). All reagents are analytical-grade and use without further purification. Ultra-pure water(Smart2Pure, ThermoFisher) was used in all experiments.

CuS/S nanocomposites preparation procedure carried out as follows: 100 mL of distilled ultra-pure water was taken in a 250 mL three-necked round bottom flask equipped with a condenser, and it was placed over a magnetic stirrer. The temperature was raised to 80°C, and then 10 mL of thiourea solution (0.2 M) was added to the water under vigorously stirred condition. After that, also 10 mL of copper acetate solution (0.1 M) was added by dripping to the solution with the view to produce copper sulfide. Solution color is started turning from the colorless to the black. Then 5 mL of thiourea solution was dripped to the system in order to react with copper acetate residues. Hereupon, like in previous procedures, 10 ml of copper chloride solution was added dropwise to the above solution to obtain sulfur nanoparticles. All these step reactions were repeated twice to produce enough amount of sample for further characterization analyses. After synthesis, obtained greenish-black precipitant were centrifuged at 4000 rpm (Rotina-380R, Germany) and dried at 50ºC during 6 h.

X-ray diffraction patterns were obtained on a MiniFlex 600 diffractometer (Rigaku, Japan) in a digital form using copper radiation. Sample analysis modes are as follows: X-ray tube voltage is 40 kV, the tube current is 15 mA, goniometer movement step is 0.02 2θ, and intensity measurement time at the point is 0.12 sec. During shooting, the sample was rotated in its plane at a speed of 60 rpm. For phase analysis, the ICCD-PDF2 Release 2016 database and the PDXL2 software has been used.

The Raman data were obtained by using a combined system Solver Spectrum (NT-MDT Spectrum Instruments, Russia), equipped with a photomultiplier tube (PMT) detector, a high-stability fast confocal laser (Rayleigh) imaging and 600/600 grating, 473 nm solid state laser excitation. In all experiments, laser power at the sample was 35 mW, and the exposure time was 60 s. Continuously tunable filters ND = 0.5 which reduce the laser intensity by 30% were also used. Without the use of a filter, the sulfur sampleis decomposed by the laser action. When using a blue laser, an error of ±4 cm^{-1} is provided.

Thermal analyses (thermogravimetry (TG) and differential scanning calorimetry (DSC)) were carried out under nitrogen with a NETZSCH 449F3A-0372 M

(NETZSCH, Germany) instrument at temperatures up to 750 °C and a heating rate of 20 K/min.

Scanning electron microscopic (SEM) examinations of the samples were carried out with a SEMQuanta 3D 200i instrument (FEI, Netherlands). Conducting carbon adhesive tape was used as a substrate for the samples.

RESULTS AND DISCUSSION

XRD analysis. Figure 1 shows the XRD patterns of the CuS/S nanocomposites. The diffraction peaks of the CuS/S nanocomposites closely matched the standard copper sulfide and sulfur peaks. It is observed that in the case of sulfur, the peaks observed at 2θ = 11.47º, 15.55º, 18.43º, 21.17º, 23.07º, 25.83º indexed as (111), (022), (202), (115), (222) and (026) planes corresponding to orthorhombic phase with space group Fddd (70) (ICCD PDF-2 card №00-064-0585). From the patterns, it is also noticed that copper sulfide particles have diffraction peaks at 2θ values 27.12º, 27.67º, 29.27º, 31.78º, 47.92º, 52.73º, 59.32º indexed as (100), (101), (102), (103), (110), (108) and (116) planes corresponding to the hexagonal covellite phase with space group P63/mmc (194) (ICCD PDF-2 card №01-078-0877). No other peaks were detected, indicating the high purity of the sample.

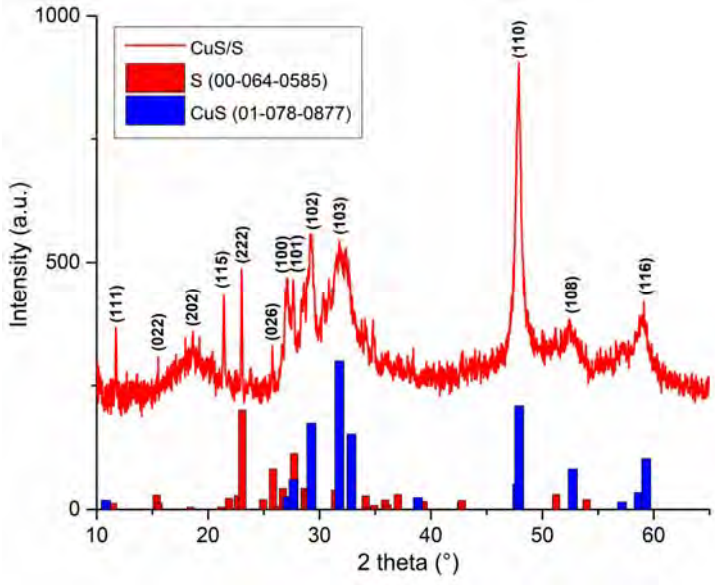

Figure 1 – XRD pattern of as-synthesized CuS/S nanocomposites by the hydrothermal route.

The average crystallite size of copper sulfide and sulfur particles in the composite was calculated by Williamson-Hall's formula as follows:

$$\Delta K = \frac{0.9}{D} + K\varepsilon\,, \qquad (1)$$

where $\Delta K = \beta cos\theta/\lambda$ and β is the instrumental corrected full width at half maximum (FWHM), θ is the Bragg's angle, λ is the wavelength of CuKα radiation (1.5406 Å), $K = 4sin\theta/\lambda$, D is the average crystallite size and ε is the lattice strain [41]. According to the noted equation, the average crystallite size of copper sulfide and sulfur particles was about 3.5 and 3.6 nm, respectively.

Raman spectroscopy analysis. A typical Raman spectrum of CuS is shown in figure 2. The peak is pronounced at 468 cm^{-1}, which corresponds to the vibrational (stretching) modes of the S–S covalent bond [42] and the much weaker peak at 260 cm^{-1} is explained by the fluctuation of the Cu–S bond [42]. In the works of Munce and Safrani et al. [43, 44], Raman spectra of covellite with the sharp band at 468 cm^{-1} which is attributed to S–S stretching vibration and a weak band at 263 cm^{-1} corresponding to A_{1g} TO mode are presented. However, according to their results, both of these peaks have been associated with the covellite phase of CuS.

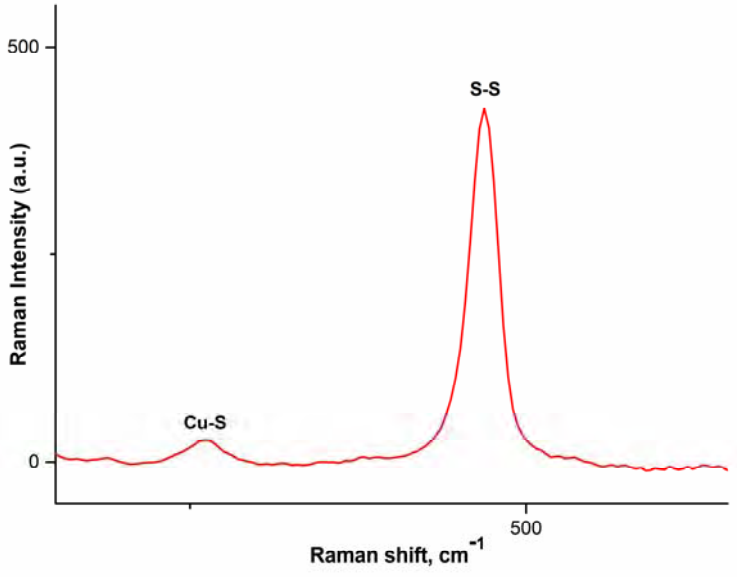

Figure 2 – Raman spectra of as-synthesized CuS/S nanocomposite

Usually, sulfur has three distinct peaks in the Raman spectrum. According to [45, 46], the main wave numbers determining sulfur are around 152, 220, and 474 cm^{-1}. However, in our case, apart from the characteristic peaks of the covellite, the sulfur peaks are not present in the Raman spectrum. This can be explained by the fact that sulfur could burn under the action of a laser beam or with the too small size of sulfur crystals, which makes it difficult to measure with Raman spectroscopy due to the phonon confinement effect [47]. Other explanations of this phenomenon are not considere since the other characterizing methods (XRD and TG-DSC) confirm the presence of sulfur in the composite material.

TG-DSC analysis. Thermal analysis of CuS/S sample was performed in a nitrogen environment, which is shown in figure 3. From the DSC curve can be seen the small endothermic effect at 115 °C, which shows the phase transformation of sulfur from S_α to S_β [48]. The decomposition proceeds in the following steps: TGA curve shows that the first loss up to 260 °C with a mass loss of around 16.16 % due to the sulfur content removal and corresponding endothermic peak emerged at 260 °C. CuS nanoparticles are desulfurized at around 450 °C to obtain the Cu_2S product [49]. According to the reaction (1), 12.29 % mass decrement is observed between 260 °C and 455 °C with small and sharp exothermic peaks, which point out 385 and 455 °C respectively.

$$2CuS \rightarrow Cu_2S + S\ . \qquad (1)$$

After 455 °C, from the curve can be seen a fluent mass decrement (12.55 %) with an exothermic peak at 525 °C. This weight reduction goes to around 720 °C and then stabilizes to a plateau. In this temperature range, the Cu_2S can decompose, forming copper and sulfur. This decomposition can be expressed by the following reaction (2):

$$Cu_2S \rightarrow 2Cu + S\ . \qquad (2)$$

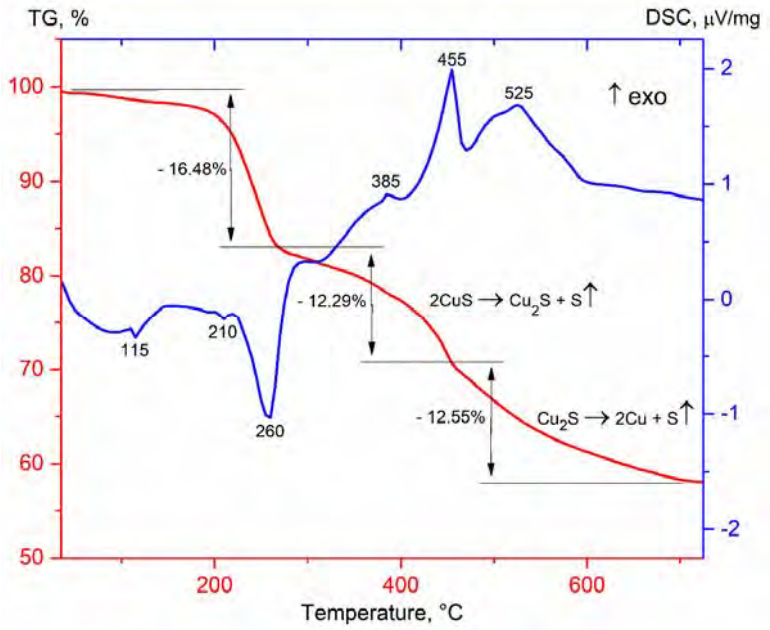

Figure 3 – TG-DSC curves of CuS/S nanocomposite sample

SEM analysis. To study the morphology of the obtained CuS/S nanocomposites, scanning electron microscopy analysis was used. In figure 4, we can see sample particles with non-uniform sizes. It can be clearly seen (see figure 4b) two shapes of particles: spherical and elongated (needle-like) ones. As Raman spectro-

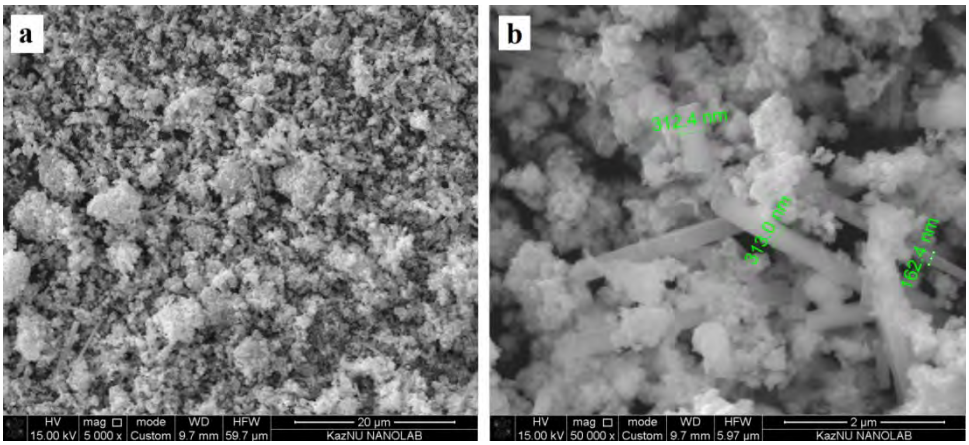

Figure 4 – SEM images of CuS/S nanocomposite: a – 5000× , b – 50 000×

scopy could not detect sulfur from the composite material, we can definitely say that it is amorphous and has a non-structured shape. In the case of CuS nanoparticles, it is observed elongated needle-likeCuS (nCuS) structures with the thickness from c.a.160 nm to 300 nm. Length of the nCuS particles exceeds their width around 20-30 times.

Conclusion. A shape-controlled hydrothermal synthesis of copper sulfide/sulfur nanocomposites is proposed in this report. XRD, Raman, TG-DSC and SEM analyses confirmed the successful formation of CuS and S nanoneedles and nanoparticles respectively. The present study could serve as a protocol for the shape-controlled synthesis of nanocomposites using the hydrothermal route, which could open a new branch of this environmentally friendly and sustainable synthetic method.

Acknowledgements.*This work was supported by the Ministry of Education and Science of Kazakhstan Republic (grants BR05234566 and AP05133115).*

REFERENCES

[1] Baláž P., Baláž M., Achimovičová M., Bujňáková Z., Dutková E. Chalcogenide mechanochemistry in materials science: insight into synthesis and applications (a review) // J. Mater. Sci. 52 (2017) 11851-11890.

[2] Ryan K.M., Cabot A., Coughlan C., Ibáñez M., Dobrozhan O., Singh A. Compound copper chalcogenide nanocrystals // Chem. Rev. 117(9) (2017) 5865-6109.

[3] Yu J., Zhang J., Liu S. Ion-Exchange Synthesis and Enhanced Visible-Light Photoactivity of CuS/ZnS Nanocomposite Hollow Spheres // J. Phys. Chem. C 114(32) (2010) 13642-13649.

[4] Baláž P., Baláž M., Dutková E., Zorkovská A., Kováč J., Hronec P., J. Kováč Jr., Čaplovičová M., Mojžiš J., Mojžišová G., Eliyas A., Kostova N.G. CdS/ZnS nanocomposites: from mechanochemical synthesis to cytotoxicity issues // Mater. Sci. Eng., C 58 (2016) 1016-1023.

[5] Lu C., Liu C., Chen R., Fang X., Xu K., Meng D. Synthesis and characterization of ZnO/ZnS/CuS ternary nanocomposites as high efficient photocatalyst in visible light // Journal of materials science-materials in electronics 27(7) (2016) 6947-6954.

[6] Nogueira A.F., Benedetti J.E., Bernardo D.R., Morais A., Bettini J. Synthesis and characterization of a quaternary nanocomposite based on TiO_2/CdS/rGO/Pt and its application in the photoreduction of CO_2 to methane under visible light // RSC Adv. 5(43) (2015) 33914-33922

[7] Habibi-Yangjeh A., Akhundia A. Facile preparation of novel quaternary g-C_3N_4/Fe_3O_4/AgI/Bi_2S_3 nanocomposites: magnetically separable visible-light-driven photocatalysts with significantly enhanced activity // RSC Adv. 6(108) (2016) 106572-106583.

[8] Habibi-Yangjeh A., Shekofteh-Gohari M. Fe_3O_4/ZnO/Ag_3VO_4/AgI nanocomposites: Quaternary magnetic photocatalysts with excellent activity in degradation of water pollutants under visible light // Sep. Purif. Technol. 166 (2016) 63-72.

[9] Dong S., Wang P., Zhai Y., Wang D. Synthesis of reduced graphene oxide-anatase TiO_2 nanocomposite and its improved photo-induced charge transfer properties // Nanoscale 3(4) (2011) 1640-1645.

[10] Pan S., Liu X. ZnS–Graphene nanocomposite: Synthesis, characterization and optical properties // J. Solid State Chem. 191 (2012) 51-56.

[11] Saranya M., Ramachandrana R., Kollub P., Jeong S.K., Grace A.N. A template-free facile approach for the synthesis of CuS–rGO nanocomposites towards enhanced photocatalytic reduction of organic contaminants and textile effluents // RSC Adv. 5(21) (2015) 15831-15840.

[12] Goel S., Chen F., Cai W.B. Synthesis and biomedical applications of copper sulfide nanoparticles: From sensors to theranostics // Small 10(4) (2014) 631-645.

[13] Suh M.P., Cho K., Han S.-H. Copper–organic framework fabricated with CuS nanoparticles: synthesis, electrical conductivity, and electrocatalytic activities for oxygen reduction reaction // Angewandte Chemie - International Edition 55(49) (2016) 15301-15305.

[14] Grozdanov I., Najdoski M. Optical and electrical properties of copper sulfide films of variable composition // J. Solid State Chem. 114(2) (1995) 469-475.

[15] Nair P.K., Nair M.T.S., Pathirana H.M.K.K., Zingaro R.A., Meyers E.A. Structure and composition of chemically deposited thin films of bismuth sulfide and copper sulfide - effect on optical and electrical properties // J. Electrochem. Soc. 140(3) (1993) 754-759.

[16] Wang H.-Y., Hua X.-W., Wu F.-G., Li B., Liu P., Gu N., Wang Z., Chen Z. Synthesis of ultrastable copper sulfide nanoclusters via trapping the reaction intermediate: potential anticancer and antibacterial applications // ACS Appl. Mater. Interfaces 7(13) (2015) 7082-7092.

[17] Yan H., Yaping W., Wenhong G., Yijing W., Lifang J., Huatang Y., Shuangxi L. Synthesis of novel CuS with hierarchical structures and its application in lithium-ion batteries // Powder Technol. 212(1) (2011) 64-68.

[18] Cheng F.M., Qi Z.Y., Xiao F.Q., Gen T.Z., Mao L.L., Sheng Q.F. Controlled synthesis of various hierarchical nanostructures of copper sulfide by a facile microwave irradiation method // Colloids and Surfaces A-physicochemical and Engineering Aspects 371(1-3) (2010) 14-21.

[19] Guangzhao M., Wenfei D., Dirk G.K., Helmuth M. Synthesis of copper sulfide nanorod arrays on molecular templates // Nano Lett. 4(2) (2004) 249-252.

[20] Guozhen S., Di C., Kaibin T., Xianming L., Liying H., Yitai Q. General synthesis of metal sulfides nanocrystallines via a simple polyol route // J. Solid State Chem. 173(1) (2003) 232-235.

[21] Reijnen L., Meester B., Lange F.D., Schoonman J., Goossens A. Comparison of Cu_xS films grown by atomic layer deposition and chemical vapor deposition // Chem. Mater. 17(10) (2005) 2724-2728.

[22] Baláž M., Zorkovská A., Urakaev F., Baláž P., Briančin J., Bujňáková Z., Achimovičová M., Gock E. Ultrafast mechanochemical synthesis of copper sulfides // RSC Adv. 6(91) (2016) 87836-87842.

[23] Saranya M., Santhosh C., Augustine S.P., Grace A.N. Synthesis and characterisation of CuS nanomaterials using hydrothermal route // J. Exp. Nanosci. 9(4) (2014) 329-336.

[24] Lu Q., Gao F., Zhao D. One-step synthesis and assembly of copper sulfide nanoparticles to nanowires, nanotubes, and nanovesicles by a simple organic amine-assisted hydrothermal process // Nano Lett. 2(7) (2002) 725-728.

[25] Wang G., Li K., Wanga B., Sua D., Park J., Ahnb H. Enhance electrochemical performance of lithium sulfur battery through a solution-based processing technique // J. Power Sources 202 (2012) 389-393.

[26] Wild M., Offer G.J., O'Neill L., Zhang T., Purkayastha R., Minton G., Marinescub M. Lithium sulfur batteries, a mechanistic review // Energy & Environmental Science 8(12) (2015) 3477-3494.

[27] Zhang S.S. Liquid electrolyte lithium/sulfur battery: Fundamental chemistry, problems, and solutions // J. Power Sources 231 (2013) 153-162.

[28] S.e. al. Sulfur Nanoparticles: Synthesis, Characterizations and their Applications // J. Mater. Environ. Sci. 4(6) (2013) 6.

[29] Ellis M.A., Ferree D.C., Funt R.C., Madden L.V. Effects of an apple scab-resistant cultivar on use patterns of inorganic and organic fungicides and economics of disease control // Plant Dis. 82(4) (1998) 428-433.

[30] Basu S., Choudhury S.R., Roy S., Goswami A. Polyethylene glycol-stabilized sulphur nanoparticles: an effective antimicrobial agent against multidrug-resistant bacteria // J. Antimicrob. Chemother. 67(5) (2012) 1134–1137.

[31] An Y.-l., Nie F., Wang Z.-y., Zhang D.-s. Preparation and characterization of realgar nanoparticles and their inhibitory effect on rat glioma cells // Int. J. Nanomed. 6 (2011) 3187-3194.

[32] Porras I. Sulfur-33 nanoparticles: A Monte Carlo study of their potential as neutron capturers for enhancing boron neutron capture therapy of cancer // Appl. Radiat. Isot. 69(12) (2011) 1838-1841.

[33] Shamsipur M., Pourmortazavi S.M., Roushani M., Kohsari I., Hajimirsadeghi S.S. Novel approach for electrochemical preparation of sulfur nanoparticles // Microchim. Acta 173(3-4) (2011) 445-451.

[34] Deshpande A.S., Khomane R.B., Vaidya B.K., Joshi R.M., Harle A.S., Kulkarni B.D. Sulfur Nanoparticles Synthesis and Characterization from H_2S Gas, Using Novel Biodegradable Iron Chelates in W/O Microemulsion // Nanoscale Research Letters 3(6) (2008) 221-229.

[35] Kouzegaran V.J., Farhadi K. Green synthesis of Sulphur Nanoparticles assisted by a herbal surfactant in aqueous solutions // Micro & Nano Lett. 12(5) (2017) 329-334.

[36] Paria S., Chaudhuri R.G. Synthesis of sulfur nanoparticles in aqueous surfactant solutions // J. Colloid Interface Sci. 343 (2010) 439–446.

[37] Xie X.-Y., Zheng W.-J., Bai Y., Liua J. Cystine modified nano-sulfur and its spectral properties // Mater. Lett. 63(16) (2009) 1374-1376.

[38] LaMer V.K., Kenyon A.S. Kinetics of the formation of monodispersed sulfur sols from thiosulfate and acid // J. Colloid Sci. 2(2) (1947) 257-264.

[39] He D., Xue P., Song D., Qu J., z. Chao Laia. Tri-Functional Copper Sulfide as Sulfur Carrier for High-Performance Lithium-Sulfur Batteries // J. Electrochem. Soc. 164(7) (2017) A1499-A1502.

[40] Karikalan N., Karthik R., Chen S.-M., Karuppiah C., Elangovan A. Sonochemical Synthesis of Sulfur Doped Reduced Graphene Oxide Supported CuS Nanoparticles for the Non-Enzymatic Glucose Sensor Applications // Sci. Rep. 7 (2017).

[41] Kalita M.P.C., Kalita A. Williamson-Hall analysis and optical properties of small sized ZnO nanocrystals // Physica E 92 (2017) 36-40.

[42] Ishii M., Shibata K., Nozaki H. Anion Distributions and Phase Transitions in $CuS_{1-x}Se_x$ (x=0-1) Studied by Raman Spectroscopy // J. Solid State Chem. 105 (1993) 504-511.

[43] Munce C.G., Parker G.K., Holt S.A., Hope G.A. A Raman spectroelectrochemical investigation of chemical bath deposited Cu_xS thin films and their modification // Colloids Surf. Physicochem. Eng. Aspects 295(1-3) (2007) 152-158.

[44] Safrani T., Joppb J., Golan Y. A comparative study of the structure and optical properties of copper sulfide thin films chemically deposited on various substrates // RSC Adv. 3(45) (2013) 23066-23074.

[45] Jaroudi O.E., Picquenard E., Gobeltz N., Demortier A., Corset J. Raman spectroscopy study of the reaction between sodium sulfide or disulfide and sulfur: identity of the species formed in solid and liquid phases // Inorg. Chem. 38(12) (1999) 2917-2923.

[46] Wang J., Chenb J., Konstantinov K., Zhaoa L., Nga S.H., Wang G.X., Guoa Z.P., Liu H.K. Sulphur-polypyrrole composite positive electrode materials for rechargeable lithium batteries // Electrochim. Acta 51(22) (2006) 4634-4638.

[47] Zuo J., Xu C., Liu Y., Qian Y. Crystallite size effects on the Raman spectra of Mn_3O_4 // Nanostructurred Materials 10(8) (1998) 1331-1335.

[48] Černošek Z., Holubová J., Černošková E., Růžička A. Sulfur – a new information on this seemingly well-known element // Journal of Non-oxide Glasses 1(1) (2009) 38-42.

[49] Saha B., Saikia J., Das G. Correlating enzyme density, conformation and activity on nanoparticle surfaces in highly functional bio-nanocomposites // The Analyst 140(2) (2015) 532-542.

Резюме

Ж. С. Шалабаев, А. Қ. Өскенбай,
П. Е. Оразбай, А. Ш. Дуйсенкулова

CuS/S НАНОКОМПОЗИТІН ГИДРОТЕРМИЯЛЫҚ ЖОЛМЕН СИНТЕЗДЕУ ЖӘНЕ СИПАТТАМАСЫ

Мыс сульфиді/күкірт негізіндегі нанокомпозиттер $Cu(CH_3COO)_2$, $CuCl_2$ және $(NH_2)_2CS$ өзара әрекеттестіру арқылы 80 °С температурасында сулы ортада гидротермиялық жолмен сәтті синтезделді.Синтезделген сынама рентгенфазалық талдау (РФТ), Раман спектроскопиясы, ТГ-ДСК және сканирлеуші электронды микроскопия (СЭМ) талдау әдістерімен сипатталды.РФТ талдауының нәтижелері бойынша CuS/S нанокомпозиттерінің дифракционды пиктері стандартты мыс сульфиді және күкірт пиктерімен толығымен сәйкес келді. Мыс сульфидінің және күкірт бөлшектерінің кристаллиттерінің орташа мөлшері сәйкесінше 3,5 және 3,6 нм құрады. ТГ-ДСК талдауларының нәтижелері композициялық материалдың құрамында 16,16% күкірт және 12,29% мыс сульфиді (ковеллит) бар екенін көрсетті.СЭМ суреттері композициялық материал екі түрлі микроқұрылымнан тұратынын көрсетті: ұзартылған ине тәрізді нанобөлшектер және құрылымдық емес агломераттар.

Түйін сөздер: мыс сульфиді, күкірт, нанокомпозит, гидротермиялық әдіс, пішінді қадағалау.

Резюме

Ж. С. Шалабаев, А. К. Оскенбай, П. Е. Оразбай, А. Ш. Дуйсенкулова

СИНТЕЗ НАНОКОМПОЗИТОВ CuS/S ГИДРОТЕРМИЧЕСКИМ ПУТЕМ И ИХ ХАРАКТЕРИСТИКА

Нанокомпозиты сульфид меди/сера были успешно синтезированы гидротермическим путем, реагируя Cu(CH3COO)2, CuCl2 и (NH2)2CS в водной среде при 80 °C. Образец после синтеза был охарактеризован с помощью дифракции рентгенофазным анализом (РФА), рамановской спектроскопии, ТГ-ДСК и сканирующей электронной микроскопии (СЭМ). Согласно результатам рентгеноструктурного анализа, дифракционные пики нанокомпозитов CuS/S близко соответствовали стандартным пикам сульфида меди и серы. Средний размер кристаллитов частиц сульфида меди и серы составлял около 3,5 и 3,6 нм соответственно.Результаты ТГ-ДСК анализа показали, что композитный материал содержит около 16,16% серы и 12,29% сульфида меди (ковеллит). СЭМ изображения показали, что композитный материал состоит из двух разных микроструктур: удлиненных игольчатых и неструктурированных агломератов.

Ключевые слова: сульфид меди, сера, нанокомпозит, гидротермический метод, контроль формы.